Journal of Chromatography A, 1216 (2009) 6789–6795

Contents lists available at ScienceDirect

Journal of Chromatography A

journal homepage: www.elsevier.com/locate/chroma

Peak shape and dispersion behavior of solutes in counter-current chromatography with a single phase

Ching-Wei Shen, Tiing Yu*

Department of Applied Chemistry, National Chiao Tung University, 1001 Ta-Hsueh Road, Hsinchu 30050, Taiwan

ARTICLE INFO

Article history:
Received 27 May 2009
Received in revised form 27 July 2009
Accepted 5 August 2009
Available online 11 August 2009

Keywords:
Counter-current chromatography
Dispersion
Diffusion
Wide-bore hydrodynamic chromatography
Nanoparticles
Rotational coiled tube
Convection peak

ABSTRACT

The dispersion behavior of solutes was investigated in a rotating flowing coiled tube. Potassium iodide, tartrazine, ascorbic acid, lysozyme, bovine serum albumin (BSA), and silver nanoparticle (AgNPs) samples were eluted in a coiled tube of counter-current chromatography (CCC) apparatus with a single phase. Apparent convection peaks of low-diffusivity solutes appeared in the static CCC tube, while Gaussian-like peaks showed up for the high-diffusivity solutes. When the rotation speed of the CCC apparatus was elevated, all solute peak widths became smaller, and the convection peaks of AgNPs and BSA were minimized and formed Gaussian-like peaks. The axial dispersions of all solutes were reduced owing to the higher radial mass transfer in the rotating CCC column. The same reasoning could also be used to rationalize other special band shapes encountered in two-phase CCC separations.

© 2009 Elsevier B.V. All rights reserved.

1. Introduction

Counter-current chromatography (CCC) is a liquid–liquid chromatographic technique without packing solid-state support for the liquid stationary phase in the separation column. The column of a J-type high-speed counter-current chromatography, one of the most common CCC apparatuses, is usually made of a coiled polytetrafluoroethylene (PTFE) tube. The tube diameter of this HSCCC is applied to various scales of separation, including analytical (I.D. = 0.8 mm), semi-preparative (I.D. = 1.6 mm), and large-scale preparation (I.D. = 2.6 mm) [1–3]. The analytical columns of smaller bores, usually operated under a higher rotational speed, provide better separation efficiency. Separations are carried out based on solute partition between the stationary and mobile phases (i.e., two-phase solvent systems). In addition, three-phase solvent systems were reported for components with a broad hydrophobic range of natural products. Separations could be done in less time [4]. Ito et al. [5,6] demonstrated particle and cell separations using CCC in a non-synchronous coil planet centrifuge. Fedotov [7] successfully fractionated micro-size particles suspended in the single phase of a J-type synchronous coil planet centrifuge. Furthermore, a single phase as the carrier in CCC was used for size-separation of micrometer particles and silica gels [8,9]. The elution of particles dispersed in the coiled PTFE column was affected by the centrifugal force and the elution speed of the carrier. Micrometer quartz-sand particles were separated into several fractions according to their sizes. Small particles (<1 μm in diameter) were collected in the first fraction of the effluent. We tried to separate nanoparticles according to their size in the single-phase CCC but did not find any promising results. However, some interesting consequences regarding peak shapes prompted us to start the current study, that is, the elution behavior of nanometer-scale particles in rotating coiled columns.

When nanoparticles were eluted in an open tube, a so-called convection peak with an extended tail appeared instead of the Gaussian-like peak usually observed in a flow injection analysis (FIA). Particles of different sizes [10] could be partially resolved in a single-phase liquid carrier, a technique named wide-bore hydrodynamic chromatography (HDC). The apparatus of the wide-bore HDC appeared similar to that of the FIA. Based on a laminar flow model, the linear velocity reaches the maximum at the center of the tube and decreases as a function of the radial coordinate during the elution. Solute molecules of low-diffusivity could not exchange fast enough in the radial direction, so as expected, a convection peak emerged at the carrier front with an extended tail. The solute profiles in wide-bore capillaries were dependent on the sample diffusion coefficient, the capillary diameter, and the linear flow rate according to computer simulations [11,12]. Nanoparticles and biomolecules were separated using HDC, with the channels grooved on a silica chip [13,14]. The separation mechanism was

* Corresponding author. Tel.: +886 3 573 1673; fax: +886 3 572 3764.
E-mail address: tyu@faculty.nctu.edu.tw (T. Yu).

0021-9673/$ – see front matter © 2009 Elsevier B.V. All rights reserved.
doi:10.1016/j.chroma.2009.08.010

based on the dispersive difference between these molecules. When the elution time was long enough for diffusion, the solute peak will eventually turn into a Gaussian profile. The diffusion coefficients of proteins and nanoparticles can be calculated from the peak widths using this technique [15–17].

In the present study, solute peak shapes and dispersions were investigated in the CCC coiled tube under rotation. Solutes of various diffusivities were eluted under different flow rates and rotation speeds of the CCC to investigate the dispersion in a semi-preparative HSCCC with single phase as the carrier.

2. Experimental

2.1. Sample preparations

Tartrazine, sodium borohydride, ascorbic acid, lysozyme, bovine serum albumin (BSA), and 11-mercaptoundecanoic acid (MUA) were all purchased from Sigma–Aldrich (St. Louis, MO, USA). Potassium iodide (KI), silver nitrate, and dipotassium phosphate were from Showa (Tokyo, Japan). Tris(hydroxymethyl)-aminomethane (Tris) was purchased from Tedia (Fairfield, OH, USA). Water was purified in a Milli-Q apparatus (Millipore, Bedford, MA, USA).

The MUA-modified silver nanoparticles (AgNPs) were synthesized in a similar way as that reported in the literature [18]. First, 5.1 mg of MUA was added into 75 ml of a freshly prepared sodium borohydride solution (20 mM). After stirring for 5 min, 75 ml of silver nitrate solution (5 mM) was added dropwise into the previous aqueous solution with vigorous stirring. The color of the clear solution initially turned light yellow and finally to dark yellow due to the formation of silver nanoparticles. After 24 h of stirring, the solution was adjusted to pH 2 by adding 0.1 M HCl, and the nanoparticles were precipitated by a centrifuge (Hermle Z323K, Wehingen, Germany) running under 6000 rpm for 10 min. The dark-brown precipitate (AgNPs) was then dispersed in a phosphate buffer (20 mM K_2HPO_4, pH 11) to obtain a 300 mg/l sample solution. The AgNPs particle size was then measured by a JSM-7401F field emission scanning electron microscope (JEOL, Tokyo, Japan). The average diameter and standard deviation were 15.8 ± 5.3 nm.

In addition, a 200 mg/l tartrazine sample was prepared by dissolving tartrazine in the phosphate buffer. Protein samples (500 mg/l) were prepared by dissolving an adequate amount of lysozyme and BSA in the Tris–HCl buffer (20 mM, pH 8). Ascorbic acid (30 mg/l) and KI (3000 mg/l) samples were prepared in de-ionized water.

2.2. CCC instrument and procedures

The chromatograph used was a Model CCC-1000 (Pharma-Tech Research, MD, USA) apparatus, mounted in a temperature-controlled oven set at 20 °C. It contained three spool-shaped column holders; only one holder was coiled with a 19 m × 1.6 mm I.D. PTFE tube (total volume 38 ml) with a β value of 0.59. Both sides of the coil were connected with a 0.8 m long × 0.8 mm I.D. PTFE tube to the pump and detector. The coiled tube was first filled up with either buffer solution or de-ionized water depending on the sample solvent. The CCC was in static mode or was set to the desired rotation speed. The same solution as the carrier was pumped into CCC in the head-to-tail mode under the desired flow rate. After sample (1 ml) injection, the effluent was monitored by a Bio-Rad Model 1801UV detector (Hercules, CA, USA) at the desired wavelengths for tartrazine (420 nm), ascorbic acid (265 nm), lysozyme (220 nm), BSA (220 nm), and AgNPs (420 nm). The KI signal was monitored by an Alltech (Deerfield, IL, USA) Model 650 conductivity detector. All elution signals were acquired using a SISC version 3.1 Chromatography Data Station (Taipei, Taiwan).

3. Results and discussion

3.1. Peak profiles in the static coiled tube

The Reynolds numbers of experiments under all six flow rates (0.5, 1.0, 1.5, 2.0, 2.5, and 3.0 ml/min) in this study were calculated. The numbers were all smaller than 100, thus laminar flows were encountered in all elutions. As generally known, the linear flow velocity $u(r)$ of a laminar flow as a function of the radial coordinate r and the tube radius a can be described by the following equation:

$$u(r) = 2u_{av}\left(1 - \frac{r^2}{a^2}\right) \quad (1)$$

where u_{av} stands for the flow average velocity. The fluid maximum velocity occurs at the center of the tube. Solute molecules existing in the center zone move faster than those close to the tube's inner wall.

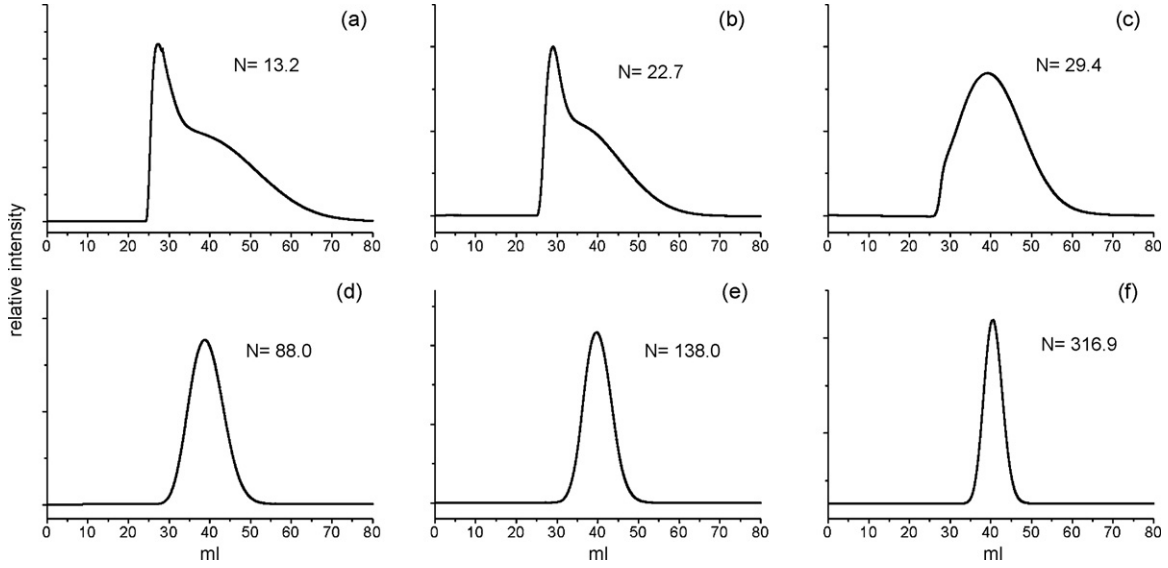

Fig. 1. Peak profiles obtained in static CCC of (a) AgNPs, (b) BSA, (c) lysozyme, (d) tartrazine, (e) ascorbic acid, and (f) KI. The flow rate was 2 ml/min, and the signals were obtained from UV–vis and a conductivity detector.

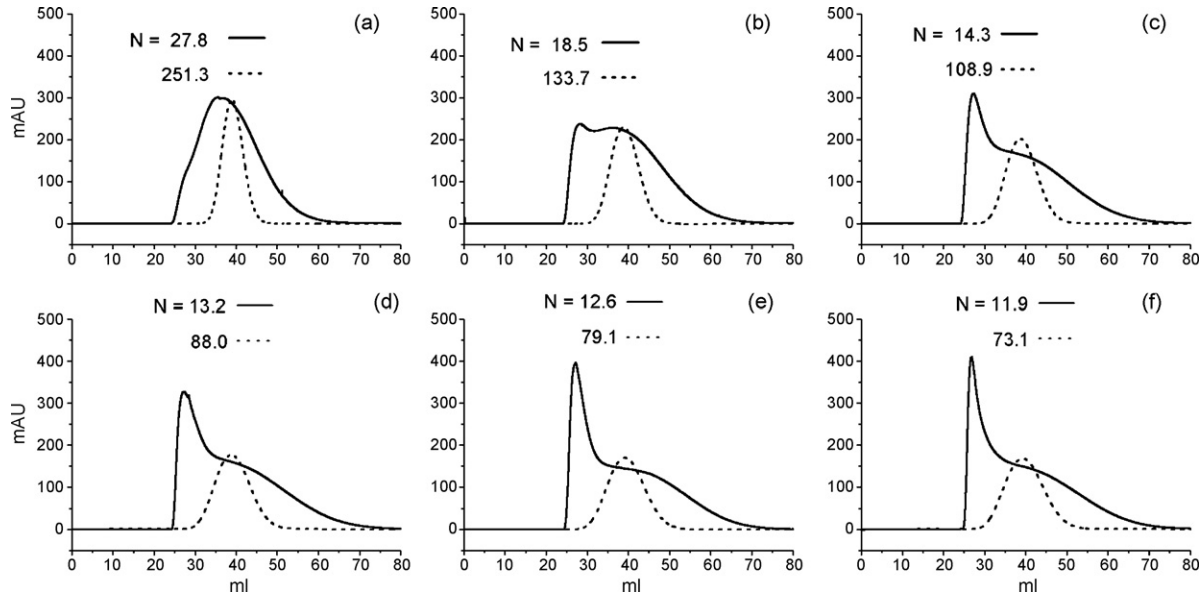

Fig. 2. Peak profiles obtained for AgNPs (solid line) and tartrazine (dash line) samples eluted in a static CCC coiled tube. The flow rate was set to (a) 0.5 ml/min, (b) 1 ml/min, (c) 1.5 ml/min, (d) 2.0 ml/min, (e) 2.5 ml/min, and (f) 3.0 ml/min.

The peak profiles can be analyzed using the classic studies done by Taylor and Aris [19–21]. The plate height H as well as the theoretical plate N can be expressed in the following equation [17]:

$$N = \frac{L}{H} = \frac{D_m \times L}{\kappa \times a^2 \times u_{av}} \quad (2)$$

where a is the tube radius, u_{av} is the average linear flow rate, D_m is the molecular diffusion coefficient, L is the tube length, and κ is the velocity profile factor related to the secondary flow effect in the radial direction. Therefore, flow rate, tube diameter, tube length, and solute diffusivity are factors that affect the N values. The N value can be obtained experimentally from the peak profile by the following equation:

$$N = \left(\frac{T}{\sigma}\right)^2 \quad (3)$$

$$\sigma = \sqrt{\frac{\int y(t-T)^2 dt}{\int y dt}} \quad (4)$$

where T is the peak mass center (in ml), y is the detection signal, t is the elution volume, and σ is the standard deviation.

All six samples were first examined under the flow rate of 2 ml/min. The peak profiles are shown in Fig. 1. The theoretical plate numbers computed by Eq. (3) were 13.2, 22.7, 29.4, 88.0, 138.0, and 316.9 for AgNPs, BSA, lysozyme, tartrazine, ascorbic acid, and KI, respectively. Golay and co-worker [22] pointed out that a Gaussian profile should be obtained when $N > 30$. The profiles of ascorbic acid, tartrazine, and KI were Gaussian with N values much greater than 30. The radial diffusivities of these solutes were relatively large, and this helped reduce the velocity disparity in the flowing tube. Accordingly, the axial dispersions of the high-diffusivity samples appeared relatively small in all experiments. The N values of AgNPs and BSA were much smaller than 30, and thus resulted in convec-

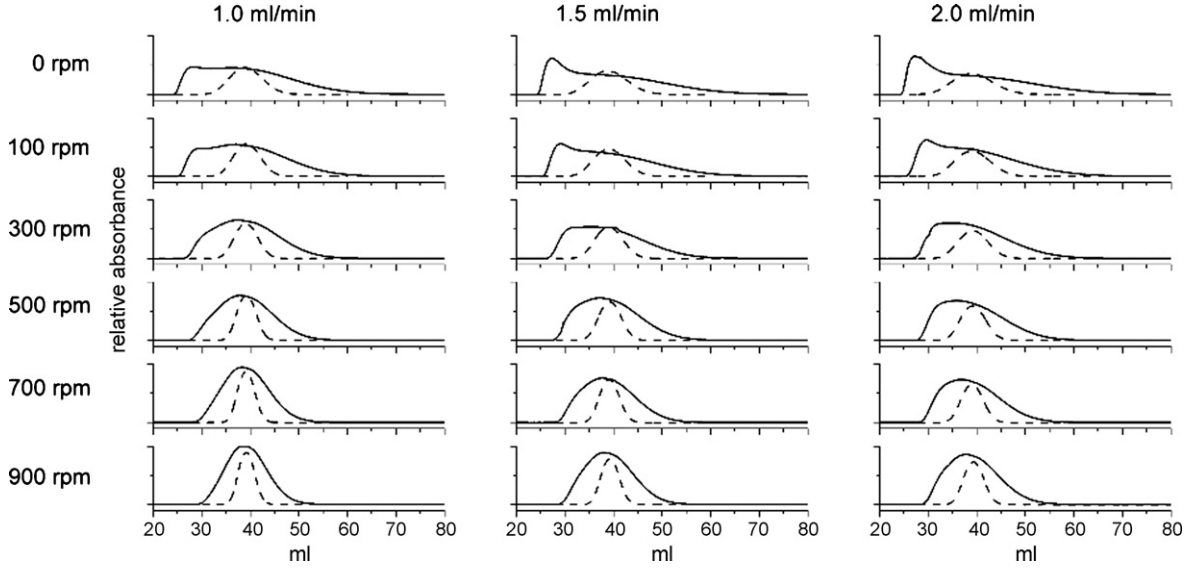

Fig. 3. Peak profiles obtained for AgNPs (solid line) and tartrazine (dash line) samples eluted in rotational CCC under 1.0, 1.5, and 2.0 ml/min. The rotational speed was set to 0, 100, 300, 500, 700, and 900 rpm.

Table 1
Peak profile data of tartrazine and AgNPs eluted in rotational CCC.

	Rotation speed (rpm)	Peak height (mAU)	Peak summit (ml)	Mass center (ml)	Calculated σ (ml)	N	Normalized σ
Tartrazine (1 ml/min)	0	230.13	38.93	39.20	3.39	133.7	1.00
	100	280.58	39.14	39.34	2.75	204.6	0.81
	300	301.07	39.07	39.17	2.40	266.4	0.71
	500	386.24	39.16	39.24	1.97	396.8	0.58
	700	435.57	39.14	39.18	1.78	484.5	0.53
	900	445.72	39.19	39.24	1.70	532.8	0.50
AgNPs (1 ml/min)	0	237.80	28.18	39.27	9.12	18.5	1.00
	100	277.40	37.08	39.22	8.00	24.0	0.88
	300	327.82	37.40	39.22	6.34	38.3	0.70
	500	385.27	37.90	39.16	5.39	52.8	0.59
	700	473.02	38.26	39.28	4.56	74.2	0.50
	900	502.73	38.47	39.37	4.08	93.1	0.45
Tartrazine (1.5 ml/min)	0	202.01	38.69	39.24	3.76	108.9	1.00
	100	234.20	38.88	39.25	3.31	140.6	0.88
	300	271.35	39.00	39.11	2.85	188.3	0.76
	500	331.25	39.20	39.27	2.32	286.5	0.62
	700	369.20	39.11	39.17	2.04	368.7	0.54
	900	390.64	39.24	39.30	1.89	432.4	0.50
AgNPs (1.5 ml/min)	0	309.59	27.28	39.02	10.33	14.3	1.00
	100	279.20	29.11	39.23	8.58	20.9	0.83
	300	271.89	35.28	39.13	7.16	29.9	0.69
	500	364.28	37.15	39.30	6.06	42.1	0.59
	700	380.17	37.74	39.15	5.20	56.7	0.50
	900	445.70	37.93	39.26	4.71	69.5	0.46
Tartrazine (2 ml/min)	0	176.29	38.82	39.30	4.19	88.0	1.00
	100	217.09	38.86	39.27	3.62	117.7	0.86
	300	237.86	39.14	39.31	3.07	164.0	0.73
	500	295.20	39.12	39.28	2.58	231.8	0.62
	700	325.76	38.98	39.07	2.27	296.2	0.54
	900	365.55	39.34	39.38	2.09	355.0	0.50
AgNPs (2 ml/min)	0	327.35	27.20	39.16	10.76	13.2	1.00
	100	312.64	29.62	39.31	8.78	20.0	0.82
	300	303.15	35.12	39.54	7.36	28.9	0.68
	500	340.80	35.88	39.25	6.26	39.3	0.58
	700	369.15	36.86	39.18	5.54	50.0	0.51
	900	428.85	37.74	39.44	5.24	56.7	0.49

tion peaks [10]. The Gaussian-like profile of lysozyme, gave a tailing peak accompanied by a very small convection shoulder. Its N value was close to 30, the criteria for forming a Gaussian peak.

All six samples were investigated under six flows. The results for the tartrazine and AgNPs samples are shown in Fig. 2. As can be seen, the Gaussian peak widths of tartrazine became greater as the flow rates became elevated. Higher linear flow rates resulted in greater expansion and larger peak widths. As the flow rate was increased for the AgNPs sample, it also allowed less time for radial diffusion; therefore, the convection peak height of this low-diffusivity solute became even greater. However, the signals of the high-diffusivity solute (tartrazine) showed no convection peak under the same flow rate. Accordingly, all AgNPs peak profiles covered wider ranges than the tartrazine samples. Although the peak summits and dispersions of all experiments were quite different, their peak mass centers all emerged at ~39 ml. Under the size-separation of silica gel in single-phase CCC, the retention volumes depended upon the particle size [9]. The invariable mass center in this study indicated that no retention or physical/chemical adsorption for all six solutes occurred in the flowing coil tubes.

3.2. Peak profiles in the rotational coiled tube

The profiles of typical Gaussian peaks (tartrazine) and convection peaks (AgNPs) at three flow rates (1.0, 1.5, and 2.0 ml/min) were investigated under five rotation speeds. The results are displayed in Fig. 3 and the relevant data are listed in Table 1. Under any given flow rate, the standard deviations of the solute peaks decreased when the rotation speed increased for either the tartrazine or the AgNPs samples. The tartrazine profiles remained Gaussian, similar to those examined in the static tube. However, the AgNPs profiles changed from the double-hump shape to a Gaussian-like as the rotation speed increased, and the peak standard deviations were reduced at the same time. Apparently, higher rotation speed resulted in lower dispersion during the elution. Under any given rotation speed, higher flow rate resulted in wider signal profiles for either tartrazine or AgNPs; similar to the results

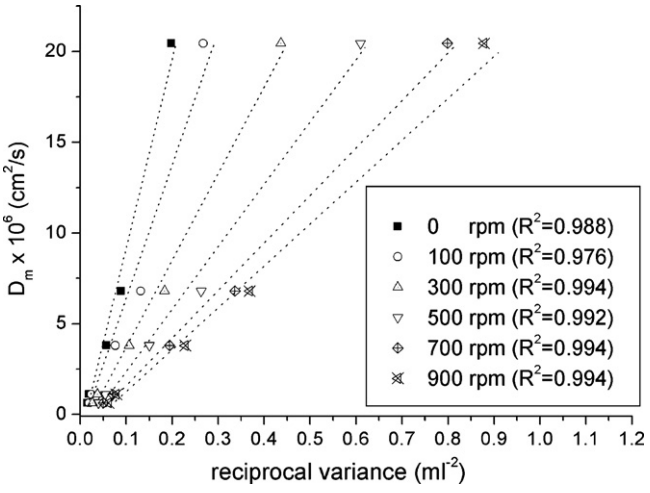

Fig. 4. The relation of reciprocal variances of solutes calculated from the experiments and their diffusion coefficients. The flow rate was 2 ml/min.

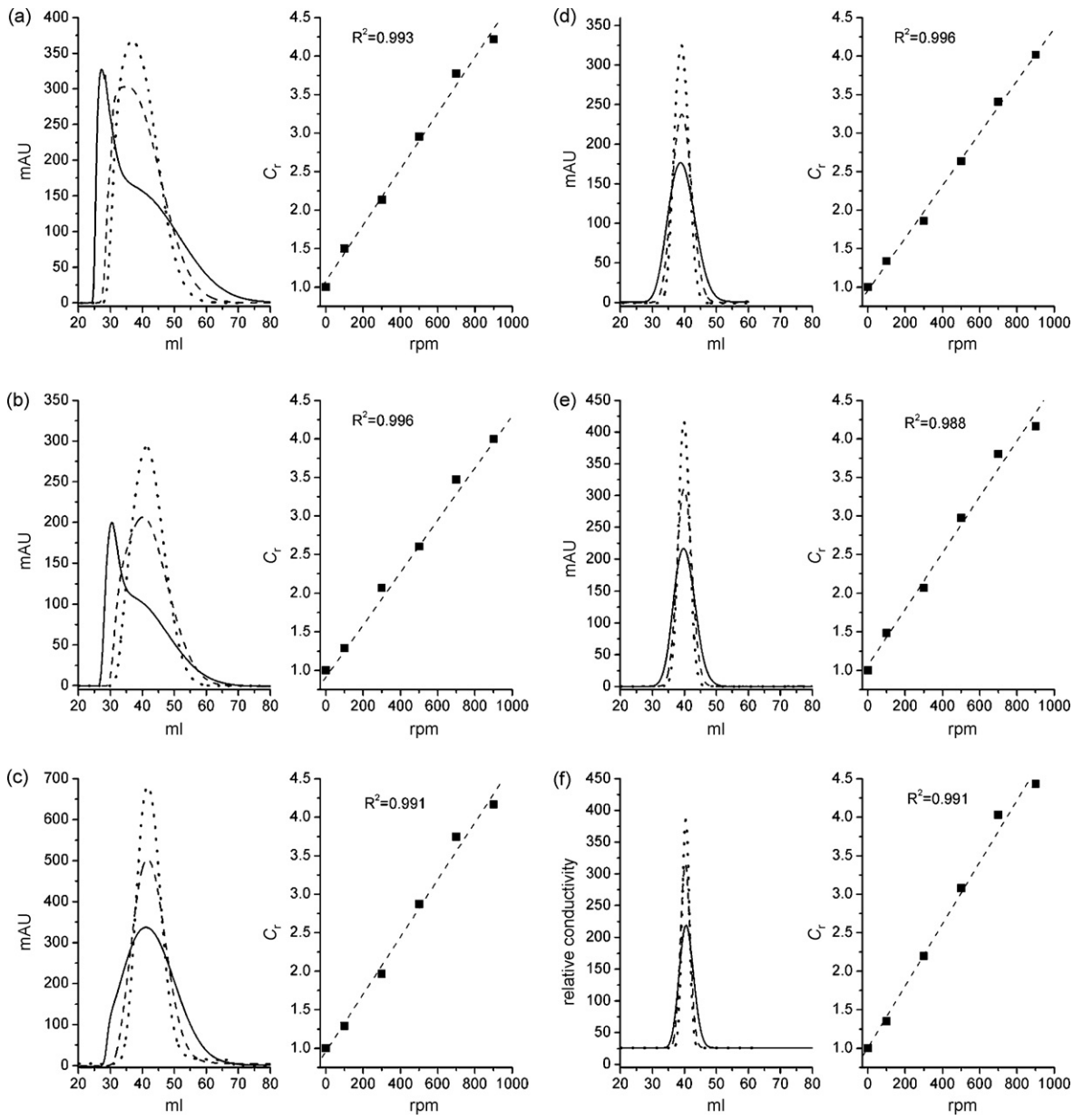

Fig. 5. Six samples: (a) AgNPs, (b) BSA, (c) lysozyme, (d) tartrazine, (e) ascorbic acid, and (f) KI. Peak profiles (left diagram) eluted in CCC of various rotation speeds: 0 rpm (solid line), 300 rpm (dash line), and 700 rpm (dot line). The flow rate was 2 ml/min. The linear relation (right diagram) of rotation parameter and rotation speed was presented, including six rotation speeds (0, 100, 300, 500, 700, and 900 rpm).

in the static CCC column. Convection peaks appeared for AgNPs under static or lower rotation speed (100 rpm). However, the profiles became Gaussian as the rotation speed increased, but their bandwidths were still greater than those of tartrazine. The effect of the flow rate on dispersion appeared to counteract the effect of the rotation speed. The peak mass centers for all experiments were again located at the elution volume ~39 ml no matter which rotation speed and flow rate were applied.

An understanding of the CCC operational mechanism is needed to explain the experimental results. It is well known that settling and mixing zones arise in the J-type CCC coiled tube under revolution. The mixing zones occur in the tube close to the center of the centrifuge. Vigorous mixing of the two immiscible phases can be observed using a stroboscope [23]. The repetitive frequency of mixing and settling zone partition was raised by speeding up the revolution. For typical examples, the process of mixing and settling zones was repetitively partitioned 13 times per second at 800 rpm and 16 times per second at 1000 rpm [23,24]. Although no direct evidence indicated the occurrence of the same mixing and settling phenomena in a single phase, mixing might still take place in the single phase owing to the sudden change of the centrifugal force. In addition, the radial mass transfer in a coiled tube has been reported to be greater than that in a straight tube because of the additional centrifugal force developed in the radial direction [25]. Accordingly, the large centrifugal force exerted on the coiled tube as a result of CCC rotation would probably further increase the radial mass transfer of solute molecules. Consequently, the resulting higher radial mass transfer would help reduce the standard deviations of both sample distributions in the flowing tube.

Standard deviations were normalized by taking the highest σ (obtained in the static tube) as 1 for each flow rate. It is interesting to explore that the normalized σ decreased almost in the same trend (see the last column in Table 1) as the rotation speed increased. The rotation speed appeared to exert the same effect

onto the sample dispersion no matter what the flow rate and sample were. This indicated that the rotational motion affected only the radial mixing of the bulk fluid but not any particular solute. Another experimental result of the six samples eluted in the same flow rate (2 ml/min) was provided. The diffusion coefficient should be proportional to reciprocal variances ($1/\sigma^2$) for a typical FIA. This relationship was examined in the CCC column under rotating. The diffusion coefficients for KI [11], ascorbic acid [26], tartrazine [27], lysozyme [28], and BSA [29] measured in aqueous solutions were reported to be 2.04×10^{-5}, 6.8×10^{-6}, 3.8×10^{-6}, 1.11×10^{-6}, and 6.38×10^{-7} (cm^2/s), respectively, in the literature. The diffusion coefficient was plotted against reciprocal variances for these five samples under rotation. Linear relationships were found, as shown in Fig. 4.

It implied that another factor that was related to the CCC rotation speed should be inserted into Eq. (2) in consideration of the rotating CCC:

$$N = \frac{c_r \times D_m \times L}{\kappa \times a^2 \times u_{av}} = \left(\frac{T}{\sigma}\right)^2 \quad (5)$$

where c_r, the rotation parameter, is dependent on the rotation speed and is assumed to be equal to 1 for the static CCC column. It can be calculated under different rotation speeds using the normalized standard deviations. In addition, all six samples were investigated to explore the correlation between c_r and the rotation speed. Each sample was eluted at the flow rate of 2 ml/min under six different rotation speeds (0–900 rpm). Peak profiles under 0, 300, and 700 rpm for all six samples are shown in Fig. 5. Convection peaks of BSA and AgNPs in the static CCC column became tailed Gaussian peaks as the rotation speed was increased. As for KI, tartrazine, and ascorbic acid, the Gaussian profiles were observed for static and rational conditions. The peak dispersion, however, decreased as the rotation speed went up. In the meantime, the rotation speed was plotted as a function of the rotation parameter (c_r). Linear relation was observed for all samples.

The average values of c_r were 1.37 at 100 rpm, 2.05 at 300 rpm, 2.85 at 500 rpm, 3.70 at 700 rpm, and 4.16 at 900 rpm. Apparently, more theoretical plates (i.e., more mixing steps) were created in the rotational coiled tube than in the static coiled tube, and thus smaller bandwidths or standard deviations could be obtained. Higher c_r value under higher rotation speed resulted in higher theoretical plates and lower peak dispersion.

3.3. Discussion on related CCC research in the literature

The experimental results demonstrated the significant effect of radial mass transfer on solute peak shape. This effect on CCC peak signals has been essentially ignored in the past. Some CCC studies are thus re-examined in the following, and the effect of radial mass transfer on separation efficiency will be considered.

Better separation efficiencies have been reported for CCC using a higher rotation speed. A higher stationary-phase retention ratio (Sf) was usually proposed as being responsible for the cause. For example, Eq. (6), derived by Berthod et al. [30], clearly shows that the separation resolution R_s of two adjacent compounds is a function of Sf and N:

$$R_s = \mathrm{Sf}\frac{\sqrt{N}}{4}\frac{K_{D2} - K_{D1}}{1 - \mathrm{Sf}[1 - (K_{D2} + K_{D1})/2]} \quad (6)$$

where K_{D1} and K_{D2} are partition coefficients for compounds 1 and 2, respectively. At constant volume in CCC, a larger bore column with better Sf would have shorter length and thus result in less plate numbers. However, the higher radial mass transfer promoted by the higher rotation speed may also contribute to better efficiency, i.e., higher N, according to our study. In other words, higher rotation speed actually promotes Sf and N simultaneously to improve the separation resolution. This may be further proven in the future by performing CCC separations under the same Sf but different rotation speeds.

With the fluid's increasing viscosity, the diffusion coefficient of the solute would be decreased; a non-diffusive peak was hence reported in small-bore glass tubes [31]. In addition, a centrifugal partition chromatography (CPC), a hydrostatic-type CCC, using the butanol–acetic acid–water system, compound L-leucyl-L-tyrosine peak with an extended tail was eluted out earlier than expected [32]. When the rotational speed was increasing, the peak then emerges at the expected time and becomes Gaussian-like. The high viscosity of this elution solvent obviously retarded the radial diffusion and resulted in a tailing convection peak. The higher rotation speed promoted radial mass transfer and eventually narrowed the peak dispersion. Aqueous two-phase solvent systems are also high-viscosity fluids used in CPC, and they are frequently applied in protein separations [33,34]. Owing to the higher viscosity of the solvent systems, thus the low diffusion coefficients of the proteins, the solute peak widths appeared to be much greater than those of other low molecular-weight solutes separated under typical low-viscosity solvents. These experiments using aqueous two-phase systems were usually performed under reasonable partition coefficients and Sf values. Accordingly, the broader peak widths cannot be explained without considering the effect of radial mass transfer.

A technique called elution-extrusion countercurrent chromatography (EECCC) was developed recently to reduce the separation time [2,35]. CCC does not require the elution of the already resolved solutes inside the retention phase by the mobile phase because it is a support-free partition chromatography. The EECCC process included classical elution (Stage I), sweeping elution (Stage II), and extrusion process (Stage III). During the extrusion process, the stationary phase was pumped into the column to carry the separated solutes out of the column with the same flow rate and rotation speed [36]. Since only the stationary phase was present in this stage, the solute dispersion behavior can be investigated using the single-phase approach in the present study. The relatively shorter elution time in Stage I should help keep the solute peak narrow. Without rotation, the solutes in the stationary phase could also be pushed out of the column by pumping the stationary phase in Stage III; however, the process would give narrower solute peaks with a rotation according to our study. Meanwhile, without rotation, the peak width of the solute pushed out with the stationary phase estimated by Eq. (5) would be twice as broad (square root of 4.16/1) of that performed under 900 rpm.

In conclusion, we investigated the shapes and dispersion of six solutes in J-type CCC. The standard deviations of all solute signals were reduced under rotational motions. The higher radial mass transfer created by the rotation was responsible for the decreased peak dispersion. Overall, the study facilitated a better understanding of CCC peak profiles under rotation.

Acknowledgment

We thank the National Science Council of Taiwan for their financial support to this research (NSC 97-2113-M-009-013-).

References

[1] F.Q. Yang, Y. Ito, J. Chromatogr. A 943 (2002) 219.
[2] A. Berthod, J.B. Friesen, T. Inui, G.F. Pauli, Anal. Chem. 79 (2007) 3371.
[3] C.F. Zanatta, E. Cuevas, F.O. Bobbio, P. Winterhalter, A.Z. Mercadante, J. Agric. Food Chem. 53 (2005) 9531.
[4] A. Yanagida, Y. Yamakawa, R. Noji, A. Oda, H. Shindo, Y. Ito, Y. Shibusawa, J. Chromatogr. A 1151 (2007) 74.
[5] Y. Ito, M. Weinstein, T. Aoki, R. Harada, E. Kimura, K. Nunogaki, Nature 212 (1966) 985.
[6] Y. Ito, P. Carmeci, I.A. Sutherland, Anal. Biochem. 94 (1979) 249.
[7] P.S. Fedotov, J. Liquid Chromatogr. Relat. Technol. 25 (2002) 2065.

[8] P.S. Fedotov, B.Y. Spivakov, V.M. Shkinev, Anal. Sci. 16 (2000) 535.
[9] O.N. Katasonova, P.S. Fedotov, B.Y. Spivakov, M.N. Filippov, J. Anal. Chem. 58 (2003) 473.
[10] C.H. Fischer, M. Giersig, J. Chromatogr. A 688 (1994) 97.
[11] M. Harada, T. Kido, T. Masudo, T. Okada, Anal. Sci. 21 (2005) 491.
[12] T. Okada, M. Harada, T. Kido, Anal. Chem. 77 (2005) 6041.
[13] E. Chmela, R. Tijssen, M. Blom, H.J.G.E. Gardeniers, A. van den Berg, Anal. Chem. 74 (2002) 3470.
[14] M.T. Blom, E. Chmela, R.E. Oosterbroek, R. Tijssen, A. van den Berg, Anal. Chem. 75 (2003) 6761.
[15] M.S. Bello, R. Rezzonico, P.G. Righetti, Science 266 (1994) 773.
[16] G. Gerhardt, R.N. Adams, Anal. Chem. 54 (1982) 2618.
[17] M. Ibrahim, G.W. Zou, J.J. Zhu, Instrum. Sci. Technol. 26 (1998) 333.
[18] W.L. Shi, Y. Sahoo, M.T. Swihart, Colloid Surf. A 246 (2004) 109.
[19] G. Taylor, Proc. R. Soc. A 219 (1953) 186.
[20] G. Taylor, Proc. R. Soc. A 223 (1954) 446.
[21] R. Aris, Proc. R. Soc. A 252 (1959) 538.
[22] J.G. Atwood, M.J.E. Golay, J. Chromatogr. 218 (1981) 97.
[23] Y. Ito, J. Chromatogr. A 1065 (2005) 145.
[24] I.A. Sutherland, J. Muytjens, M. Prins, P. Wood, J. Liquid Chromatogr. Relat. Technol. 23 (2000) 2259.
[25] M.J.E. Golay, J. Chromatogr. 186 (1979) 341.
[26] G.W. Zou, Z. Liu, C.X. Wang, Anal. Chim. Acta 350 (1997) 359.
[27] A. Abad, S.C. Cardona, J.I. Torregrosa, F. Lopez, J. Navarro-Laboulais, J. Math. Chem. 38 (2005) 541.
[28] D. Brune, S. Kim, Proc. Natl. Acad. Sci. U.S.A. 90 (1993) 3835.
[29] C.T. Culbertson, S.C. Jacobson, J.M. Ramsey, Talanta 56 (2002) 365.
[30] A. Berthod, S. Ignatova, I.A. Sutherland, J. Chromatogr. A 1216 (2009) 4169.
[31] T. Korenaga, F.H. Shen, H. Yoshida, T. Takahashi, Bull. Chem. Soc. Jpn. 62 (1989) 1492.
[32] A. Berthod, Comprehensive Analytical Chemistry, vol. 38, Elsevier, Amsterdam, 2002.
[33] K. Shinomiya, Y. Kabasawa, K. Yanagidaira, H. Sasaki, M. Muto, T. Okada, Y. Ito, J. Chromatogr. A 1005 (2003) 103.
[34] M.J. Ruiz-Angel, V. Pino, S. Carda-Broch, A. Berthod, J. Chromatogr. A 1151 (2007) 65.
[35] A. Berthod, J. Chromatogr. A 1126 (2006) 347.
[36] Y.B. Lu, R. Liu, A. Berthod, Y.J. Pan, J. Chromatogr. A 1181 (2008) 33.